SINERGI Vol. 30, No. 2, June 2026: 605-616
http://publikasi.mercubuana.ac.id/index.php/sinergi
http://doi.org/10.22441/sinergi.2026.2.023

Design and optimization of an electric screw propeller vehicle chassis using a BBNN-GA hybrid approach

Mohammad Khoirul Effendi*, Muhammad Ghazy Rizqi Fahada, Harus Laksana Guntur
Department of Mechanical Engineering, Faculty of Industrial Technology and System Engineering, Institut Teknologi Sepuluh Nopember, Indonesia

Abstract
Electric screw propeller vehicles represent an innovative solution for traversing difficult environments such as peat soil, particularly for fresh fruit bunch (FFB) transportation in the palm oil industry. However, the unique propulsion mechanism and demanding operational conditions impose significant structural challenges on the vehicle chassis, requiring a design that is both robust and lightweight to support electric vehicle efficiency. This study focuses on the design and optimization of a chassis for an electric screw-propelled vehicle for FFB transport operating on peat soil terrain. Advanced computational intelligence techniques, namely a Back Propagation Neural Network (BPNN) and a Genetic Algorithm (GA), are employed. The BPNN predicts key structural responses, including equivalent stress, fatigue life, safety factor, and weight, with high accuracy based on variations in material type and beam thickness. Furthermore, the GA utilizes these predictions to optimize the design. The optimized results show excellent agreement with finite element simulations, with deviations of only 3.47% in stress, 2.31% in fatigue life, 1.19% in safety factor, and 0.31% in weight, confirming the high predictive accuracy of the hybrid BPNN–GA model. The optimized chassis achieves a balanced trade-off between structural strength and light weight efficiency while remaining within allowable design limits. To the authors' knowledge, this study represents the first application of a hybrid BPNN–GA approach for optimizing a screw-propeller vehicle chassis operating on peat soil terrain, offering a novel computational strategy for lightweight and reliable electric vehicle design in soft-terrain environments.

Keywords:
Back Propagation Neural Network;
Chassis;
Electric Screw Propeller Vehicle;
Finite Element Method;
Genetic Algorithm;

Article History:
Received: September 19, 2025
Revised: December 19, 2025
Accepted: December 30, 2025
Published: June 8, 2026

Corresponding Author:
Mohammad Khoirul Effendi
Department of Mechanical Engineering, Faculty of Industrial Technology and System Engineering, Institut Teknologi Sepuluh Nopember, Indonesia
Email:
khoirul_effendi@me.its.ac.id

INTRODUCTION

Transportation systems play a critical role in supporting communities, particularly in regions characterized by challenging terrains such as peatlands. Peat soil can absorb up to 13 times its own weight in water, resulting in an extremely low bulk density, typically ranging from 0.1 to 0.2 [1]. This characteristic substantially reduces its bearing capacity, making peat a soft, highly compressible substrate composed largely of partially decomposed organic matter with high porosity and water content. Conventional wheeled vehicles exert contact pressures that often exceed the load-bearing capability of peat soils, causing the wheels to sink or become stuck, thus impeding mobility across such terrain.

In this context, screw-propeller vehicles offer a promising alternative for transportation across peatlands, particularly in agricultural applications such as palm oil logistics. The propeller features a large contact area between the propeller wheel and the ground, enabling these vehicles to easily navigate soils with low bulk densities, such as those found in peatlands. Screw-propelled vehicles also exhibit

amphibious capabilities, allowing operation across transitional environments involving land, mud, and shallow water [2]. Screw-propelled vehicles, attributed to a British inventor named Richard Love, are commonly used in various agricultural fields. Their unique propulsion system relies on two parallel cylinders, each equipped with helical blades, that rotate in opposite directions. This counter-rotation generates non-holonomic constraint motion between the helical blades and the terrain [3]. The advent of the Fordson Snow Tractor and other amphibious screw-propelled vehicles have significantly expanded the ability to traverse challenging terrains such as ice, snow, mud, sand, and marshes, surpassing the limitations of conventional tracked or wheeled vehicles. [4]. Because of those advantages, screw-propelled vehicles represent a novel multi-terrain platform with considerable potential in military, rescue, and extreme environment applications, owing to its exceptional adaptability and maneuverability [5].

Furthermore, screw wheels have a structural design well-suited for overcoming transitional environments between land and water, including both terrestrial and aquatic areas [6]. With advancements in computational mechanics and artificial intelligence, vehicle chassis design can now be evaluated and optimized using simulation-based approaches, significantly reducing development time and cost [7]. These advancements have enabled researchers to more effectively address the automotive industry's increasing demand for weight reduction in heavy motor vehicle chassis frames and associated structural components. To accomplish such lightweighting objectives, a wide range of optimization techniques has been progressively adopted. Contemporary freight and vehicle structures are typically designed to ensure high strength, load-carrying capacity, and structural rigidity while simultaneously incorporating lightweight materials [8]. As a result, lightweight design has become a central focus in modern automotive engineering and a key strategy for driving innovation and achieving sustainable development [9].

In automotive structural design, fundamental performance requirements include sufficient stiffness, particularly bending and torsional stiffness, along with adequate safety factors under normal operating conditions [10]. These design considerations are particularly relevant for biomimicry-inspired structures and complex geometries, which facilitate the systematic construction of an expanded theoretical design space for lightweight chassis systems. At its core, this methodology seeks optimal combinations of material selection and geometric configuration to meet target performance criteria while minimizing constraints, such as cost or weight [11]. Optimization has also grown significantly due to the need for improved performance and cost-efficiency. Techniques like genetic algorithms have seen increased the structural engineering projects for optimizing material distribution and weight reduction [12]. Structural optimization is therefore crucial in fields such as engineering, architecture, and product design, as it aims to find the most effective combinations of materials and shapes to achieve the desired performance while minimizing costs or constraints [13].

This approach signifies a fundamental shift away from traditional trial-and-error design approaches toward the use of algorithm-driven, systematic methodologies for solving complex structural problems. Contemporary optimization frameworks are closely integrated with the Finite Element Method (FEM) [14], which serves as a core analytical tool for evaluating structural responses under various loading conditions. Over the past few decades, there has been a growing trend towards the use of computational tools and advanced numerical methods for predicting the behavior of solid materials. These techniques are particularly valuable in solid and structural mechanics, where they are widely used to model deformation, internal stress distributions, fatigue behavior, and others in a broad range of applications, including the development and optimization of novel structural systems, such as screw-propeller vehicle chassis designs [15].

Recent research on screw-propeller vehicles has focused on kinematic feasibility and terrain interaction. In 2017, He and Long applied CAD and FEM concepts to validate a screw-propeller vehicle, although their work lacked an optimization method [2]. Similarly, in early 2025, Shi and Wang used the Discrete Element Method (DEM) to examine the kinematics of a multi-road screw vehicle; however, their analysis was constrained to terrain interaction and did not address the structural integrity of the chassis [5]. Various lightweighting strategies have been explored for vehicle chassis design through traditional and material-based optimization approaches. In early 2025, Tomasi achieved an 8–10% weight reduction in industrial vehicles by substituting composite materials using FEM [7]. Likewise, Galos and Sutcliffe reduced the mass of a truck trailer frame through structural optimization, resulting in a 7.8% lighter frame; however, their approach relied on conventional

methods rather than predictive AI modeling [12]. While computational intelligence has shown great promise in automotive design, Liao successfully integrated BPNN and GA with topology optimization for a passenger car chassis, achieving a 10.4% mass reduction while maintaining stiffness in 2024. However, such advanced hybrid AI methodologies have not yet been applied to the unique structural and dynamic challenges of electric screw-propelled vehicles operating on soft peat soils. Consequently, there is a distinct research gap in applying intelligent optimization to this specific vehicle class [9]. Using computational methods, a chassis frame is expected to withstand both static and dynamic loads. Therefore, the selection of chassis materials primarily depends on achieving high tensile strength while maintaining low weight, with manufacturers generally favoring options that are lightweight, cost-effective, safe, and recyclable. [16] This study addresses this gap by employing the hybrid BPNN-GA approach.

The main objective of this paper is to evaluate the performance of an electric screw-propelled vehicle chassis by analyzing different materials and beam thicknesses for the design of a ladder-frame chassis. The research is conducted using the Finite Element Method (FEM), followed by Backpropagation Neural Network (BPNN) modeling and Genetic Algorithm (GA) optimization. This study seeks to establish a versatile optimization methodology for chassis structures, offering a dependable framework for the future development of electric off-road vehicles. This study is pioneering in its application of a hybrid BPNN–GA approach for optimizing screw-propeller vehicle chassis on peat soil terrain, presenting an innovative computational strategy for designing lightweight and reliable electric vehicles for soft-terrain environments.

METHOD

This study was conducted using simulation and optimization techniques, specifically employing the FEM, BPNN, and GA. The BPNN model comprises input, hidden, and output layers, each featuring multiple interconnected neurons. The bias and weight of each neuron in these layers represent the connections between the input and output layers of the network. During the training of the BPNN model, the bias and weight of each neuron were adjusted using an error function to gradually minimize the error. The ideal network configuration, which achieved the lowest mean squared error (MSE), response prediction error, and goal function value, was selected as the optimal BPNN model. Developing a BPNN model involves the following steps: (a) selecting an appropriate training function and conducting training, testing, and validation, and (b) designing the BPNN network by setting the modeling parameters.

The parameters include variations in hidden layers and neurons, stopping criteria or maximum iterations, learning rate, and activation functions for both hidden and output layers. Additionally, the GA is a population-based metaheuristic technique. The GA begins by generating an initial population of random solutions, which are then evaluated based on a fitness function derived from the BPNN's performance. Through iterative processes of selection, crossover, and mutation, the GA evolves the population toward optimal solutions. The optimized outcomes from the combined BPNN-GA model are subsequently validated using FEM simulations in ANSYS to provide a reliable verification framework. This integration ensures that the model predictions align with the physical simulations, thereby reinforcing the credibility of the hybrid approach for solving complex optimization problems in engineering contexts.

The software tools used in this study were ANSYS 2022 R2 and MATLAB 2023B. Finite element analysis performed in ANSYS demonstrated that the system could withstand various loading conditions under full load without experiencing permanent deformation; specifically, the von-Mises stress remained well below the material's yield stress [17]. For the machine-learning based optimization, modeling is required to optimize material properties for both single-objective and multi-objective scenarios [18]. The overall research process is summarized in the flowchart presented in Figure 1, with the vehicle chassis specifications listed in Table 1.

Data and Parameter

The electric screw-propeller vehicle (E-SPV) chassis can be designed with multiple input parameters, such as material type and beam thickness. In this study, four different materials and seven selectable beam thicknesses were considered as design parameters. Finite Element Analysis (FEA) conducted in ANSYS 2022 R2

Table 1. Vehicle Chassis Specification

Parameter	Value
Overall Length	3855 mm
Overall Width	1930 mm
Max. Payload	1000 kg
Vehicle Gross Weight	±1600 kg
Estimated Usage	15 Years

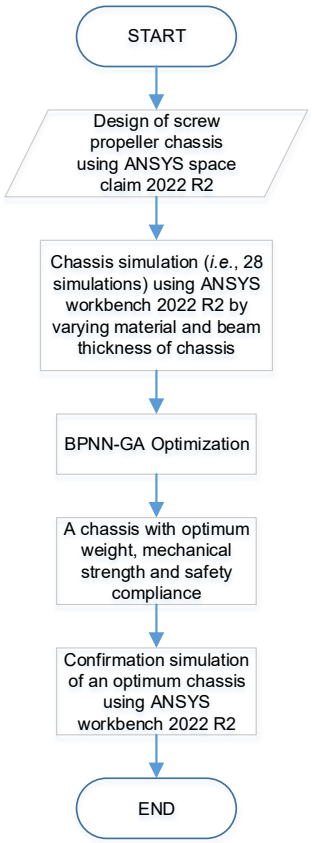

Figure 1. Research Flowchart Diagram

Finite element simulations later generated multiple output results for each parameter combination. These outputs were then used as inputs for the subsequent optimization process using the BPNN-GA approach. The parameter values used in this process are summarized in Table 2.

Finite Element Method

In the past, the dimensions of automobile components were primarily determined by conventional engineering methods based on the principles of strength of materials. Over the last few decades, the exponential increase in computational power has enabled detailed structural analysis of complex systems using various numerical techniques. Among these, the FEM has gained widespread popularity for structural analysis [19]. Three-dimensional FEM is widely used in engineering and physics to solve complex problems [20].

Table 2. The level of chassis optimization parameter

Parameters	Units	Value
Material	-	ASTM A53-A, ASTM A283-D, SS400, Aluminum A 6061
Beam Thickness	mm	3, 3.25, 3.5, 3.75, 4, 4.25, and 4,5

In this study, simulations were conducted using ANSYS 2022 R2. Static analyses were performed to determine equivalent stress, fatigue life cycle, and safety factor. The E-SPV chassis utilized rectangular hollow beams, and the mass was automatically calculated within the ANSYS geometry interface. Four different materials were evaluated, and the design of the chassis is illustrated in Figure 2.

The simulation generated results based on material selection and beam thickness. The materials investigated, namely ASTM A53 Grade A, ASTM A283 Grade D, Stainless Steel 400, and Aluminum Alloy 6061, were modeled as linear elastic and isotropic. Mechanical properties and fatigue data (S–N curves) were obtained from the ANSYS material library. The model was discretized using solid tetrahedral elements, selected for their ability to accurately capture complex joint geometries. A grid independence study was conducted by progressively refining the mesh from coarse to fine resolution to ensure the most suitable number of nodes and elements for accurate analysis [21]. At each refinement level, the maximum total deformation and maximum von-Mises stress values were monitored. Convergence was achieved when the variation between successive refinements dropped below 5%.

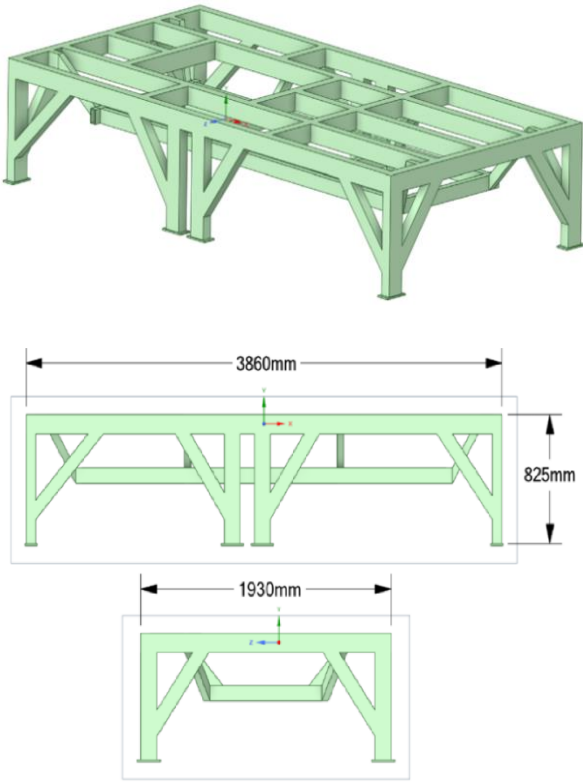

Figure 2. Electric Screw Propeller Vehicle Chassis Geometry

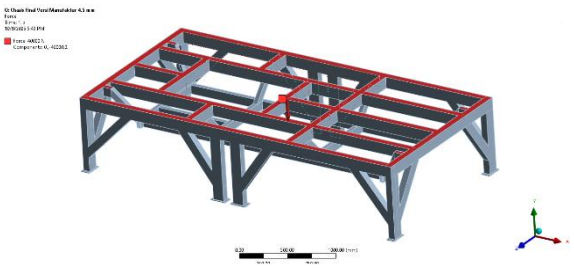

Figure 3 Finite Element Analysis Simulation Image for Electric Screw Propeller Vehicle

The optimal element size was determined to be 4 mm, with an average skewness of 0.404, which represents a balance between accuracy and computational cost. Boundary conditions were applied by fixing the wheel hub mounting regions to restrict all translational and rotational degrees of freedom, thereby simulating fully constrained ground contact. The analysis neglected the effects of welding joints, material imperfections, and corrosion, assuming ideal material behavior without degradation or residual stress.

The complete chassis model consists of 4,600,000 nodes and 2,300,000 elements, and the simulation was conducted at a 1:1 scale. The purpose of this finite element analysis (FEA) is to evaluate whether the chassis is able to withstand a load of 4,000 kg and to estimate its lifespan based on a usage rate of four cycles per day. The simulation process is already illustrated previously, while the load settings used in the analysis are pictured in Figure 3.

The FEA provided results including maximum equivalent stress, safety factor, fatigue life, and chassis weight. For each material–thickness combination, a static structural simulation was performed using identical loading and boundary conditions. These four output responses derived from ANSYS, namely the maximum equivalent stress, safety factor, estimated fatigue life, and chassis weight, are documented and summarized in Table 3. These 28 data points constitute the input dataset for the subsequent BPNN training. These results serve as the baseline for the optimization process; the finite element method was employed because full-scale prototyping of all 28 geometrical combinations is impractical and cost prohibitive. FEA allows for the prediction of stress fields, safety factors, and fatigue life with sufficient accuracy for structural decision-making.

Multi-Objective Optimization via BPNN-GA

Neural Network is a powerful tool for solving complex optimization and prediction problems. Metaheuristic algorithms, which often offer higher performance and lower computational requirements compared to deterministic methods, have been successfully applied to various optimization tasks [22, 23, 24]. To further demonstrate the industrial applicability of the GA-BPNN prediction model, it has been implemented in real-world product development [25]. A standard BPNN architecture consists of an input layer, one or more hidden layers, and an output layer [26].

The GA is widely used for multi-objective mechanical structure optimization [27]. As a representative nature-inspired metaheuristic, GA simulates natural genetic mechanisms and biological evolution. Its main advantages include robustness, simplicity, versatility, and suitability for parallel and distributed processing [28]. The optimization framework in this study integrates BPNN for predictive modeling with GA for search optimization, effectively combining the strengths of both approaches.

1. Back Propagation Neural Network Modeling
   - The chassis parameters, specifically material type and beam thickness, serve as the input features for the neural network
   - Simulation results, including equivalent stress, fatigue life, mass, and safety factor, are used to train the neural network to predict structural responses.
   - The dataset is divided into training (70%), validation (15%), and test (15%) sets to ensure effective model generalization.
   - The neural network parameters, including the number of hidden layers, neurons per hidden layer, stopping criteria (or maximum iterations), and activation functions for the hidden and output layers, are determined.
   - The trained BPNN patterns and objective functions are extracted and integrated into the subsequent GA optimization process.
2. Genetic Algorithm Optimization
   - The BPNN serves as the objective function

Table 3. The output value that generates from the FEA simulation result

Material	Beam Thickness (mm)	Max Equivalent Stress (MPa)	Safety Factor	Life Cycle (Days)	Weight (kg)
ASTM A53 Grade A	3 – 4.5	177.38 – 374.32	0.21-1.30	996-14574	470-591
ASTM A283 Grade D	3 – 4.5	157.95 – 371.32	0.23-1.31	1001-14614	467-588
Stainless Steel 400	3 – 4.5	158.75 – 375.72	0.21-1.29	1002-14553	472-592
Aluminum Alloy 6061	3 – 4.5	158.10 – 393.76	0.09-1.30	682-14592	166-209

Table 4 Constraints of GA Optimization

Parameter	Constraint
Equivalent Stress	$\sigma_{max} \leq \sigma_{yield}$
Life Cycle	≥ 15 years
Safety Factor	≥ 1.2
Chassis Weight	≤ 600 Kg
Material	ASTM A283 D
Beam Thickness	3 – 4.5 mm

- The GA searches for parameter combinations that maximize life cycle and safety factor while minimizing equivalent stress and chassis weight.
- This BPNN-GA approach effectively manages the trade-off between structural performance and stability within a complex search space.

Following these steps, the method generates the most optimized chassis parameters and predicts the corresponding performance using a fitness function derived from four objective functions

$$Minimize\ f(x) = Obj_1 + Obj_2 + Obj_3 + Obj_4 \quad (1)$$

Where Obj_1 is the objective function for equivalent stress, Obj_2 for fatigue life, Obj_3 for safety factor, and Obj_4 for weight, subject to the constrains defined in Table 4. The formulation of f(x) is designed to balance conflicting mechanical objectives, seeking a design that minimizes stress and weight while maximizing structural integrity. Table 4 imposes the necessary physical constraints on this optimization process, ensuring that any converged solution not only satisfies the mathematical fitness function but also adheres to the safety standards and yield limits of the ASTM A283 D material.

RESULTS AND DISCUSSION

The influence of material type and beam thickness on total chassis weight was analyzed using a multi-factor Analysis of Variance (ANOVA) in Minitab 21, with the results presented in Table 5. Both parameters demonstrated a significant effect on weight, with p-values < 0.05 for all factors. The ANOVA coefficients confirm that increasing beam thickness leads to higher chassis weight, whereas material selection significantly affects mass characteristics due to variations in density. This statistical validation reinforces the sensitivity of the FEA-based weight results to both geometry and material properties, ensuring reliable input data for subsequent neural network training and optimization. The BPNN's predicted data, presented in Figures 4 through 7, were compared with the original FEM results for maximum equivalent stress, fatigue life, safety factor, and chassis weight. This comparison produces the predicted values of the BPNN responses based on the original simulation data.

Table 5. ANOVA of Inputs values generated from FEA simulation results

Source	df	Sum of Square	Mean Square	P-Value	Conclusion
A-Material	3	626439	208813	<0.001	Significant
B-Beam Thickness	6	31404	5234	<0.001	Significant
AB	18	3485	193.61	<0.001	Significant
Error	18	1322657	73480.94		
Total	27	661329			

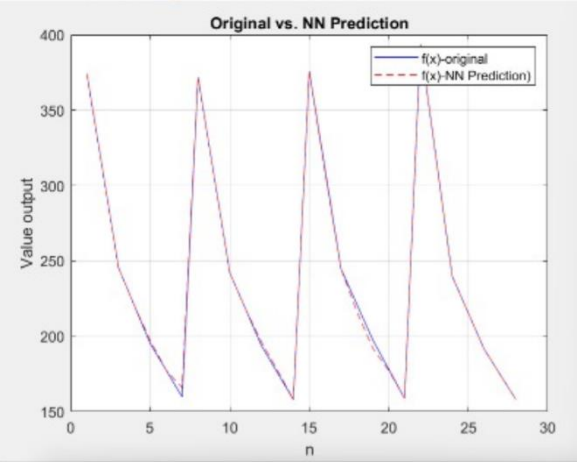

Figure 4. Prediction of Neural Network Result of Equivalent Stress Maximum

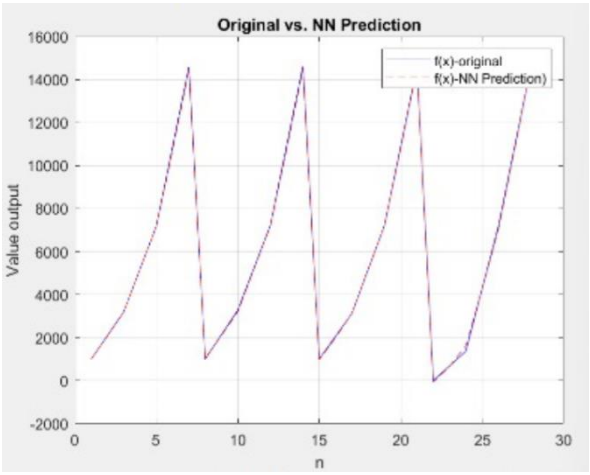

Figure 5. Prediction of Neural Network Result of Life Cycle

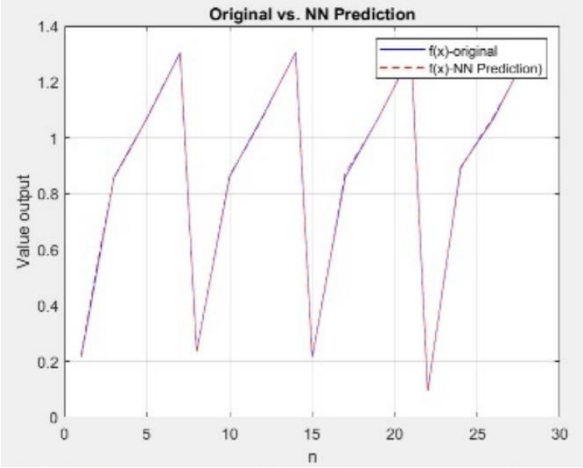

Figure 6. Prediction of Neural Network Result of Safety Factor

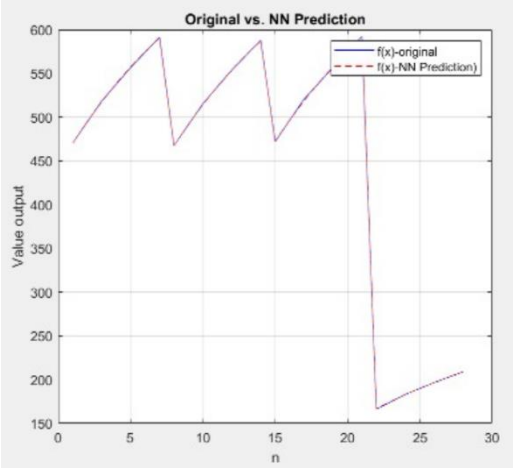

Figure 7. Prediction of Neural Network Result of Chassis Weight

All four outputs were predicted with errors below 4% using the parameter settings shown in Table 6. The prediction errors between the original FEA data and the BPNN outputs are summarized in Table 8. Figures 4 through 7 illustrate the neural network's predicted results. Using these BPNN results, the GA optimization was executed in MATLAB 2023b, with fitness values plotted against iterations (50, 100, 300, and 1000 iterations) to observe convergence. The BPNN output data were normalized prior to analysis, and Figure 8 demonstrates the distribution of one of these outputs. To ensure the selection of the most robust network, each model was generated using 10 repetitions, with the best-performing model selected as the optimal configuration. The parameter settings for the GA are shown in Table 6, the optimal results are presented in Table 7, and the prediction errors between the original FEA data and the BPNN predictions are summarized in Table 8. The regression performance of the developed BPNN exhibits excellent statistical reliability. With the final selected architecture parameters, the resulting data and error metrics are summarized in Table 8 During training, the network achieved a correlation coefficient of R = 0.99781, indicating that the predicted values closely indicating that the predicted values closely matched the target outputs with a nearly ideal regression line (slope ≈ 1, intercept ≈ 0). The validation phase maintained strong generalization capability with R = 0.99886, confirming that the model performs effectively without overfitting. Although there were slight variations in data composition and performance metrics across the 10 repetitions, the final model was selected based on the lowest calculated Mean Square Error (MSE). The Mean Squared Error (MSE) is employed to quantitatively assess the predictive accuracy of the developed model.

It represents the average of the squared deviations between the observed values (Y_i) and the predicted values ($\hat{Y}_i$), as expressed by the following equation:

$$MSE = \frac{1}{n}\sum_{i=1}^{n}(Y_i - \hat{Y}_i)^2 \quad (2)$$

To ensure reproducibility, transparency, and clarity in the optimization framework, all critical GA settings, using the roulette wheel selection scheme, are presented in Table 9. This provides a comprehensive overview of the setup that guided specifically designed to prevent premature convergence and ensure a robust search of the design space.

Table 6. Parameter utilized in BPNN modeling

Parameters	Value
Variation of hidden layers and neuron in the hidden layer	1-8 and 1-10
Six stopping criteria were employed using MATLAB's default settings. The iteration of the BPPN is halted when the first criterion is met.	(a) the number of epochs (1000 epochs) (b) time limit (determined by user) (c) performance (0) (d) gradient value (1e-07) (e) Mu (1e+10) (f) validation check (6)
Variation of activation function	Hardlim, Hardlims, Purelin, Satlin, Logsig, Tansig
Training Function	Levenberg-Marquardt
Data for training: testing: validation	70% : 15% : 15%

Table 7. Final Selected Architecture

Parameters	Eq. Stress	Life Cycle	SF	Weight
Hidden Layer	4	8	1	1
Neuron	6	3	5	3
Activation	tansig, purelin	tansig, purelin	tansig, purelin	tansig, purelin

The comparative analysis of different generation counts (50, 100, 300, and 1000) demonstrates that the optimization consistently converged to the same solution, typically between the 7th and 9th generations. This indicates that increasing the number of generations beyond 50 did not significantly affect the final optimized result, confirming the robustness and efficiency of the asearch parameters. This explanation is given in Figure 9.

To further validate the approach, the GA was also implemented using a tournament selection scheme. Similar results were obtained, with convergence occurring between the 7th and 11th generations and leading to the same optimal material selection and beam thickness for the chassis. These findings confirm that neither the choice of selection method (roulette wheel versus tournament) nor the total number of generations substantially influences the final optimization outcome. Both methods reliably converge to the same optimal solution within a narrow range of generations, highlighting the stability and consistency of the optimization framework. Consequently, the results of the optimization from GA via the roulette wheel method can thus be considered conclusive.

The optimization results using the BPNN-GA method indicate that ASTM A283 Grade D is the optimal material, paired with a beam thickness of 4.5 mm. This combination yields a maximum stress of 152.47 MPa, which, although relatively high, remains within safe limits with a safety factor of 1.33. The predicted fatigue life under these conditions is 14,439 days. Additionally, the chassis weight is approximately 585.97 kg, which is considered reasonable given its robust dimensions of 4.8 m x 1.9 m. These findings confirm that this configuration represents the most optimized set of parameters for the manufacturing process.

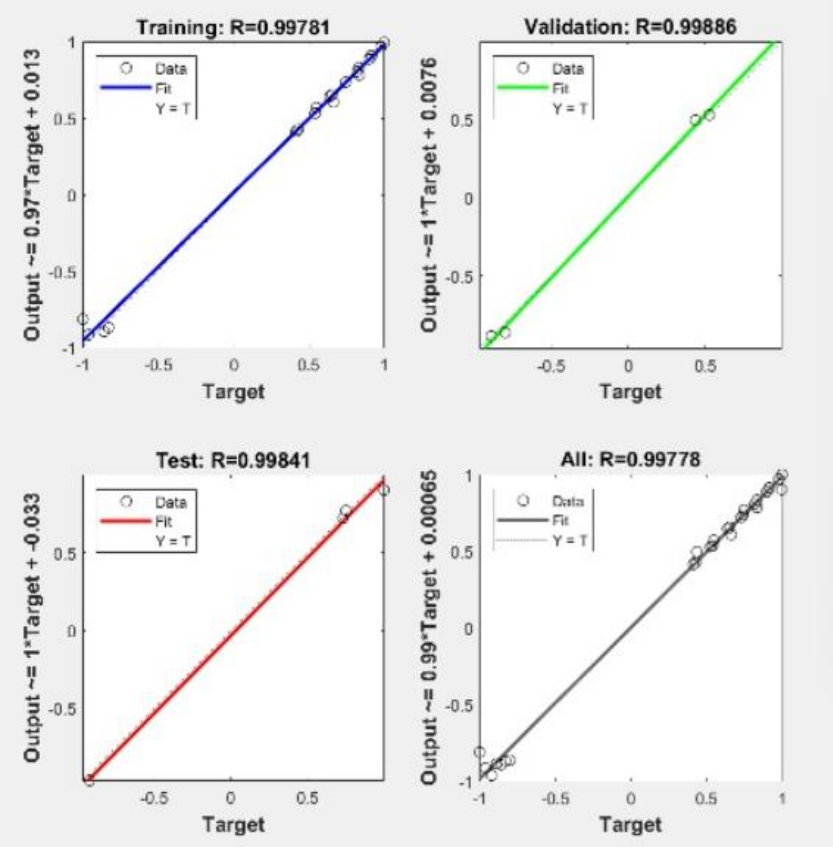

Figure 8. Regression Training Performance of BPNN Model

Table 8. Result of BPNN with Original Data and Predicted Data

n	Material	Beam Thickness (mm)	Eq. Stress (MPa)			Life Cycle (Days)			Safety Factor			Weight (Kg)		
			Ori	Pred	Error %	Ori	Pred	Error %	Ori	Pred	Error %	Ori	Pred	Error %
1		3	374.32	373.11	0.01	996	993	0.03	0.214	0.2	0.01	470.5	475	0.04
2		3.25	309.81	310.33	0.06	2098	2091	0.07	0.54	0.52	0.01	494.5	497.1	0.03
3	ASTM	3.5	245.3	247.54	0.02	3200	3189	0.11	0.86	0.85	0.01	518.4	519.3	0.01
4	A53	3.75	220.16	223.42	0.03	5192	5190	0.01	0.97	0.94	0.01	537.6	539.8	0.02
5	Grade A	4	195.02	199.3	0.05	7183	7192	0.08	1.07	1.04	0.01	556.8	560.2	0.03
6		4.25	177.39	179.2	0.02	10879	10891	0.12	1.19	1.17	0.01	574.2	580.3	0.06
7		4.5	159.75	159.1	0.01	14574	14590	0.16	1.31	1.3	0.01	591.6	600.3	0.09
8		3	371.72	369.4	0.02	1001	1014	0.13	0.24	0.25	0.01	467.5	469.3	0.02
9		3.25	306.9	307.66	0.01	2140	2157	0.18	0.55	0.58	0.01	491.4	495.3	0.04
10	ASTM	3.5	242.08	245.92	0.04	3278	3300	0.23	0.86	0.9	0.01	515.3	521.2	0.06
11	A283	3.75	217.84	219.41	0.02	5248	5256	0.08	0.97	1	0.01	534.6	538.1	0.03
12	Grade D	4	193.61	192.9	0.01	7219	7211	0.07	1.08	1.1	0.01	553.9	555	0.01
13		4.25	175.78	175.45	0.01	10916	11052	1.36	1.19	1.21	0.01	570.9	572.7	0.02
14		4.5	157.95	158	0.01	14614	14894	2.80	1.30	1.31	0.01	587.8	590.4	0.03
15		3	375.72	381.4	0.06	1002	998	0.03	0.21	0.21	0.01	472	474	0.02
16		3.25	310.2	314.42	0.04	2057	2046	0.12	0.54	0.53	0.01	496.4	499.9	0.03
17	Structur	3.5	244.68	247.43	0.03	3113	3094	0.19	0.86	0.85	0.01	520.7	525.7	0.05
18	al Steel	3.75	221.14	223.77	0.03	5155	5134	0.21	0.97	0.96	0.01	538.8	545	0.06
19		4	197.6	200.1	0.02	7198	7175	0.23	1.07	1.06	0.01	556.8	564.2	0.07
20		4.25	178.17	178.25	0.01	10875	10837	0.39	1.18	1.17	0.01	574.6	578.3	0.04
21		4.5	158.75	156.4	0.02	14553	14499	0.54	1.3	1.28	0.01	592.3	592.4	0.01
22		3	393.76	398.67	0.05	1	1	0	0.1	0.09	0.01	166	175.2	0.09
23		3.25	316.75	321.04	0.04	682	650	0.32	0.5	0.5	0	174.5	180.3	0.06
24	Aluminu	3.5	239.73	243.41	0.04	1364	1299	0.65	0.9	0.9	0	182.9	185.4	0.02
25	m Alloy	3.75	215.67	217.8	0.02	4266	4202	0.64	0.98	0.98	0	189.7	191.4	0.02
26		4	191.6	192.2	0.01	7169	7106	0.63	1.07	1.05	0.01	196.5	197.4	0.01
27		4.25	174.85	176.1	0.02	10880	10801	0.79	1.19	1.17	0.01	202.6	206.3	0.04
28		4.5	158.1	160	0.01	14592	14497	0.95	1.30	1.28	0.01	208.8	215.3	0.07
	MSE				0.001			0.005			0.001			0.001

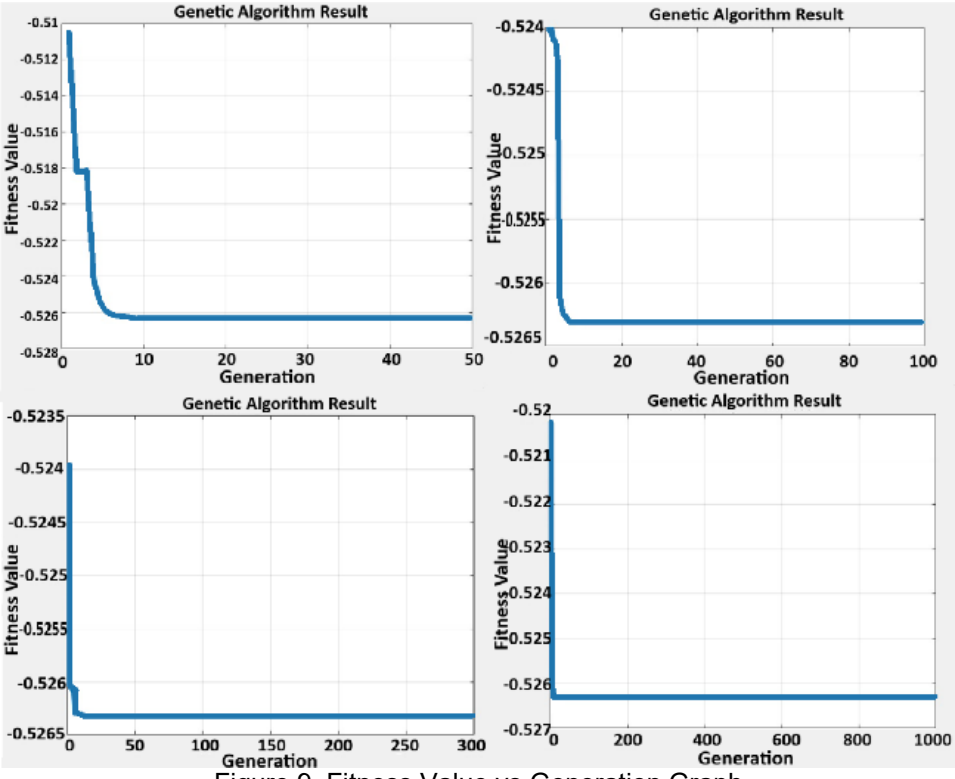

Figure 9. Fitness Value vs Generation Graph

Table 9. Parameter utilized in Genetic Algorithm Optimization method

Parameters	Value
Population Size	100
Mutation Rate	0.05
Chromosome Number	2
Crossover Method	Uniform
Selection Method	Roulette Wheel
Stopping Criteria using Max Generation	50, 100, 300, and 1000

A comparison between the BPNN–GA optimization results and the FEM–ANSYS analysis reveals excellent agreement, confirming the reliability of the proposed surrogate-based optimization framework. The deviations between the two methods are minimal: 3.47% in equivalent stress, –2.31% in fatigue life, 1.19% in safety factor, and 0.31% in total chassis weight. These small discrepancies indicate that the BPNN–GA model effectively replicates FEM response trends while significantly reducing computational effort. Overall, the hybrid model exhibits strong predictive fidelity and offers a reliable alternative to conventional FEM analysis for early-stage design and optimization.

CONCLUSION

This study presents a comprehensive analysis of an electric screw-propeller vehicle (E-SPV) chassis, integrating a BPNN-GA approach to determine the optimal combination of material and beam thickness. All four output parameters, including equivalent stress, fatigue life, safety factor, and weight, were predicted using the BPNN model, achieving mean squared error (MSE) values below 10^{-5}. The GA optimization identified ASTM A283 Grade D with a beam thickness of 4.5 mm as the optimal input. The resulting outputs include a maximum equivalent stress of 152.47 MPa, a safety factor of 1.33, a life cycle of 14,439 days and a chassis weight of 585.97 kg.

This study effectively demonstrates the success of a hybrid computational framework that integrates FEM, BPNN, and GA to optimize the chassis of an E-SPV. The findings confirm that the BPNN-GA approach adeptly addresses the complex trade-offs between minimizing chassis weight and maximizing structural durability. It achieves high-fidelity performance predictions with significantly reduced computational costs compared to traditional iterative FEA. While this study establishes a robust baseline for static structural optimization, the results are currently limited by idealized material behavior and static loading conditions. Future research should expand this methodology to dynamic scenarios, specifically exploring transient loads, fatigue under variable amplitude loading, and environmental factors such as corrosion in peat soil environments. This will further enhance the long-term reliability of the vehicle in harsh terrains.

ACKNOWLEDGMENT

The author would like to thanks *Badan Pengelola Dana Perkebunan Kelapa Sawit* (BPDPKS) for providing Research Grant number PRJ-155/DPKS/2024.

REFERENCES

[1] A. Khoerani, D. Amalia, and S. Alexsander, “Analysis of peat soil testing errors based on its characteristics and appropriate recommendation of peat soil testing,” *E3S Web of Conferences*, vol. 429, p. 04018, 2023, doi: 10.1051/e3sconf/202342904018.

[2] Y. Kai, P. Xu, H. Lin, C. Sun, M. Zhao, and G. Du, “CSUB: Numerical Investigations and Hydrodynamic Analysis of a Screw Propulsor for Underwater Benthic Vehicles,” *Journal of Ocean Engineering and Science*, vol. 13, no. 8, Aug. 2025, doi: 10.3390/jmse13081500.

[3] Y. Kai, P. Xu, H. Lin, C. Sun, M. Zhao, and G. Du, “CSUB: Design and modeling of an autonomous screw-driven amphibious vehicle,” *Journal of Ocean Engineering and Science*, vol. 10, no. 6, pp. 1031–1045, Dec. 2025, doi: 10.1016/j.joes.2025.07.003.

[4] J. Villacrés, M. Barczyk, and M. Lipsett, “Literature review on Archimedean screw propulsion for off-road vehicles,” *Journal of Terramechanics*, vol. 108, pp. 47–57, Aug. 2023, doi: 10.1016/j.jterra.2023.05.001.

[5] S. Shi and D. Wang, “Mechanism Design and Performance Analysis of Multi-Road Screw-Propelled Vehicle Based on DEM–MBD Coupling,” *Journal of Field Robotics*, vol. 42, no. 7, pp. 3853–3876, Oct. 2025, doi: 10.1002/rob.22600.

[6] J.-H. Bae, C.-H. Bae, S.-H. Jin, M.-G. Lee, S.-H. Park, and G.-R. Cho, “Advancements in Amphibious Reconnaissance Robots with Screw Wheel Propulsion,” *Journal of Korea Robotics Society*, vol. 20, pp. 94–103, Feb. 2025, doi: 10.7746/jkros.2025.20.1.094.

[7] I. Tomasi, S. Grandi, and L. Solazzi, “Implementation of Composite Materials for an Industrial Vehicle Component: A Design Approach,” *Journal of Composites Science*,

vol. 9, no. 4, p. 168, Apr. 2025, doi: 10.3390/jcs9040168.
[8] X. Wang, S. Yuan, W. Sun, W. Hao, X. Zhang, and Z. Yang, “Analysis and Validation of Lightweight Carriage Structures Using Basalt Fiber Composites,” *Materials*, vol. 17, no. 23, p. 5723, Jan. 2024, doi: 10.3390/ma17235723.
[9] S. Liao, L. Zhong, and L. Yi, “Enhancing Vehicle Lightweight Design Process with Genetic Algorithm-Optimized BP Neural Network and Topology Optimization: A Comprehensive Study,” 2024. doi: 10.20944/preprints202402.0474.v1.
[10] T. Homsnit, S. Kongwat, K. Ruangjirakit, P. Noykanna, T. Thuengsuk, and P. Jongpradist, “Optimizing stiffness and lightweight design of composite monocoque sandwich structure for electric heavy quadricycle.,” *Latin American Journal of Solids & Structures*, vol. 20, no. 3, p. 1, Apr. 2023, doi: 10.1590/1679-78257537.
[11] A. Hamza, K. Bousnina, I. Dridi, and N. Ben Yahia, “Design for Additive Manufacturing (DfAM) in the Automobile Industry,” in *Advances in Additive Manufacturing: Materials, Processes, and Applications II*, M. Soula, N. Ben Moussa, A. Trabelsi, N. Ben Yahia, F. Ghanem, and I. Dridi, Eds., Cham: Springer Nature Switzerland, 2025, pp. 231–243.
[12] G. M. Azanaw, “Design Optimization in Structural Engineering: A Systematic Review of Computational Techniques and Real-World Applications,” *American Journal of Mechanical and Materials Engineering*, vol. 9, no. 1, pp. 1–19, Jan. 2025, doi: 10.11648/j.ajmme.20250901.11.
[13] V. Goodarzimehr, J. L. J. Pereira, and N. Khodadadi, “MOSRS: An engineering multi-objective optimization through Einsteinian concept,” *PLOS ONE*, vol. 20, no. 7, p. e0328005, Jul. 2025, doi: 10.1371/journal.pone.0328005.
[14] A. Agarwal and L. Mthembu, “Structural Analysis and Optimization of Heavy Vehicle Chassis Using Aluminium P100/6061 Al and Al GA 7-230 MMC,” *Processes*, vol. 10, no. 2, p. 320, Feb. 2022, doi: 10.3390/pr10020320.
[15] A. F. Carvalho Alves, B. P. Ferreira, and F. M. Andrade Pires, “Multi-scale optimization of PC/ABS polymer blends: Microstructural design for superior toughness, strength, and weight efficiency,” *Finite Elements in Analysis and Design*, vol. 251, p. 104407, Oct. 2025, doi: 10.1016/j.finel.2025.104407.
[16] K. Dubey, B. Pathak, B. Singh, P. Rathore, and S. Yadav, “Mechanical strength study of Off-Road vehicle chassis body materials,” *Materials Today: Proceedings*, vol. 46, Apr. 2021, doi: 10.1016/j.matpr.2021.04.147.
[17] A. Mishra and A. K. Sahu, “Design Analysis and Optimization of an All-Terrain Vehicle (ATV),” *International Journal of Engineering Research & Technology*, vol. 10, no. 1, Jan. 2021, doi: 10.17577/IJERTV10IS010120.
[18] P. Xu, Y. Ma, W. Lu, M. Li, W. Zhao, and Z. Dai, “Multi-objective optimization in machine learning assisted materials design and discovery,” *Journal of Materials Informatics*, vol. 5, no. 2, p. N/A-N/A, Mar. 2025, doi: 10.20517/jmi.2024.108.
[19] S. De et al., “Lightweight Chassis Design of Hybrid Trucks Considering Multiple Road Conditions and Constraints,” *World Electric Vehicle Journal*, vol. 12, no. 1, p. 3, Mar. 2021, doi: 10.3390/wevj12010003.
[20] Y. Yao, X. Zhao, L. Chen, Y. Gu, and T. Zhou, “Reduced-integration hexahedral finite element for static and vibration analysis of micropolar continuum,” *Finite Elements in Analysis and Design*, vol. 251, p. 104412, Oct. 2025, doi: 10.1016/j.finel.2025.104412.
[21] M. Lee, G. Park, C. Park, and C. Kim, “Improvement of Grid Independence Test for Computational Fluid Dynamics Model of Building Based on Grid Resolution,” *Advances in Civil Engineering*, vol. 2020, no. 1, p. 8827936, 2020, doi: 10.1155/2020/8827936.
[22] R.-E. Precup, R.-C. David, R.-C. Roman, E. M. Petriu, and A.-I. Szedlak-Stinean, “Slime Mould Algorithm-Based Tuning of Cost-Effective Fuzzy Controllers for Servo Systems,” *International Journal of Computational Intelligence Systems*, vol. 14, no. 1, pp. 1042–1052, Mar. 2021, doi: 10.2991/ijcis.d.210309.001.
[23] Z. Iklima et al., "Defect classification of radius shaping in the tire curing process using Fine-Tuned Deep Neural Network." *Sinergi (Indonesia)*, vol. 26, no. 3, pp. 335-342, Oct. 2022, doi:10.22441/sinergi.2022. 3.009.
[24] G. Priyandoko et al., “Diagnosis of induction motor bearing defect using discrete wavelet transform and artificial neural network,” *Sinergi (Indonesia)*, vol. 25, no. 1, pp. 33-42, 2021, doi: 10.22441/sinergi.2021.1.005
[25] Y. Wu, D. Wu, M. Fei, H. Sørensen, Y. Ren, and J. Mou, “Application of GA-BPNN on estimating the flow rate of a centrifugal pump,” *Engineering Applications of Artificial Intelligence*, vol. 119, no. C, Mar. 2023, doi: 10.1016/j.engappai.2022. 105738.
[26] X. Xiao, J.-J. Kim, M.-P. Hong, S. Yang, and Y.-S. Kim, “RSM and BPNN Modeling in

Incremental Sheet Forming Process for AA5052 Sheet: Multi-Objective Optimization Using Genetic Algorithm," *Metals*, vol. 10, no. 8, p. 1003, Aug. 2020, doi: 10.3390/met10081003.

[27] Y. Sun et al., "Multi-Objective Optimization Design of Ladle Refractory Lining Based on Genetic Algorithm," *Frontiers in Bioengineering and Biotechnology*, vol. 10, Jun. 2022, doi: 10.3389/fbioe.2022.900655.

[28] J. Zhang and S. Qu, "Optimization of Backpropagation Neural Network under the Adaptive Genetic Algorithm," *Complexity*, vol. 2021, no. 1, p. 1718234, 2021, doi: 10.1155/2021/1718234.